Three- continuum states

Pierre Descouvemont

Three-alpha continuum states

Pierre Descouvemont †

Physique Nucléaire Théorique et Physique Mathématique, CP229
Université Libre de Bruxelles (ULB), B1050 Brussels, Belgium

Abstract. We investigate three-α continuum states in the hyperspherical formalism for $J = 0^+$ and $J = 2^+$. Two different types of $\alpha+\alpha$ interactions are used: the shallow Ali-Bodmer potential and the deep potential of Buck *et al.* We determine the 3α phase shifts up to $E = 6$ MeV, in parallel with an analysis of resonances in the framework of the Complex Scaling method. We show that shallow potentials provide additional narrow resonances, in contrast with experimental data. Deep potentials, however, only give rise to broad resonances, and are more consistent with the data.

PACS numbers: 21.60.Gx, 25.70.Ef, 24.10.Cn

1. Introduction

The ^{12}C spectroscopy below the 3α threshold is well known since many years (see Ref. [1] and references therein). The 0^+ ground state and the 2^+ first excited state ($E_x = 4.44$ MeV) have been investigated in many experimental and theoretical works, and their properties are now well established. The situation, however, is very different above the 3α threshold. In the continuum region, the second 0^+ state at $E_x = 7.65$ MeV plays a very important role in nuclear physics and in astrophysics. This state cannot be reproduced in standard [2, 3] or in no-core [4] shell model calculations. The 0^+_2 state is known to have a well-developed cluster structure and has been successfully described by α cluster models [5, 6, 7, 8, 9]. Fermionic molecular dynamics (FMD) calculations [10] also reproduce the 0^+_2 resonance provided that α-cluster structures are introduced in the FMD basis.

Historically, the interest for the 0^+_2 state started with the prediction of Hoyle [11] that a resonance with zero angular momentum should exist just above the $\alpha+^8$Be threshold to explain the ^{12}C abundance in the Universe. Soon after this suggestion, the 0^+_2 resonance, called the "Hoyle state", was observed experimentally 375 keV above the 3α threshold [12, 13]. In astrophysics, the determination of the triple α reaction rate at typical He-burning temperatures [14] is directly related to the properties of the Hoyle state (energy, α and γ widths). Although recently challenged by CDCC calculations [15], the 3α reaction rate is believed to be well understood.

† Directeur de Recherches FNRS

In nuclear physics the interest for the 0_2^+ structure was recently revived by its interpretation as a dilute cluster gas state of three weakly interacting α particles [16]. The analysis of electron inelastic scattering data [17], as well as cluster calculations [9] suggest a large radius of the 0_2^+ state, which reduces the overlap between the α particles. This leads to the idea of a new form of nuclear matter, in analogy with the Bose-Einstein condensates [16].

In the theoretical viewpoint, it seems well established that the Hoyle state presents an α+^{8}Be cluster structure [9, 18]. This form of α clustering is expected in light nuclei close to the α breakup threshold [19], and has been observed in many nuclei (see references in Ref. [7]). The specificity of the ^{12}C nucleus is that ^{8}Be, the other constituent of the α+^{8}Be system, presents itself an α cluster structure. Based on this interpretation of the 0_2^+ state as a bandhead of a $K = 0^+$ rotational band, microscopic cluster models [8, 9, 18] predict the existence of a 2^+ member at an energy of about $2 \sim 3$ MeV above the 3α threshold. This result is supported by the FMD [10] and by a non-microscopic 3α model [20]. This state is expected to be broad ($\Gamma \sim 1$ MeV) and may overlap with other resonances.

Historically, the experimental search for a 2^+ broad resonance is recent. Due to its specific structure, the observation of such resonance is extremely difficult. Some evidence for a 2^+ broad level was reported by Itoh *et al.* [21] near $E_\alpha \approx 9 - 10$ MeV, though not widely accepted. More recently, the situation was clarified, and a possible 2^+ resonance at $E_\alpha = 9.6 \pm 0.1$ MeV with $\Gamma = 0.6$ MeV was observed by Freer *et al.* [22]. These properties are in fair agreement with predictions of microscopic cluster models [9, 18].

The theoretical description of the $\alpha + \alpha$ system is well mastered in microscopic as well as in non-microscopic models. Microscopic theories [23] are based on a nucleon-nucleon interaction and take an exact account of the Pauli principle. In non-microscopic approaches [24], the structure of the α particle is neglected, and the Pauli principle is approximated by an appropriate choice of the $\alpha+\alpha$ potential. However, the extension of these models, which reproduce the properties of the $\alpha + \alpha$ phase shifts in a wide energy range, is not yet satisfactory for the 3α system. Microscopic approaches fail to describe accurately the $\alpha + \alpha$ and $\alpha + \alpha + \alpha$ systems with the same nucleon-nucleon interaction [25]. With a NN potential that reproduces the $\alpha + \alpha$ phase shifts, the ^{12}C ground-state is overbound. This was interpreted in Ref. [25] as a need for a three-body force. The situation is even more complex in non-microscopic theories, based on an $\alpha+\alpha$ potential. Although highly accurate potentials exist in the literature, their application to ^{12}C is still unclear, even for the ground state (see Refs. [26, 27]).

The aim of the present work is to investigate the 3α continuum in a non-microscopic approach. In the literature, this problem is usually tackled by using approximate methods to describe resonances. This can be done, for example, with the Complex Scaling Method (CSM, see Ref. [28]) or with the Analytic Continuation in the Coupling Constant (ACCC, see Ref. [29]) method. Here, we go beyond these approximations and also determine the triple α phase shifts. Recently, we have extended the hyperspherical

formalism [30] to three-body continuum states by implementing the R-matrix theory with a Lagrange basis [31]. Although the hyperspherical theory is known to converge slowly in the continuum [32, 33, 31], it provides genuine 3-body phase shifts. The model was applied in Ref. [31] to the 3-body $\alpha+n+n$ phase shifts, and suggests the existence of broad 0^+ and 1^- resonances in the low-energy spectrum of ^{6}He. The determination of phase shifts provides a coherent approach to continuum properties. It complements approximate methods by providing the wave functions not only at resonance energies, but also off resonances. Of course, resonances predicted by approximate methods should be reflected in the phase shifts. A combined approach therefore offers a rather complete picture of the continuum.

In Section 2, we briefly review the current literature on the subject. Section 3 is devoted to the models used here. We give the main properties of the hyperspherical method associated with the R-matrix theory. We also give an outline of the CSM, used as a complement to the 3α phase shifts. Results are shown in Section 4, where we use two different $\alpha+\alpha$ potentials, and compare resonance properties derived from the CSM with values extracted from the 3-body phase shifts. Conclusions and outlook are presented in Section 5.

2. Brief overview of the literature

2.1. Theoretical works

The literature concerning ^{12}C is very abundant, and it is of course impossible to review all papers on the subject. Here we essentially focus on works aimed at investigating states above the 3α threshold. In a theoretical point of view, the Hamiltonian is given by

$$H=\sum_{i=1}^{3}T_i+\sum_{i>j=1}^{3}V_{\alpha\alpha}(|\boldsymbol{r}_i-\boldsymbol{r}_j|)+V_{\alpha\alpha\alpha}(\boldsymbol{r}_1,\boldsymbol{r}_2,\boldsymbol{r}_3), \tag{1}$$

where T_i is the kinetic energy of α particle i with coordinate $\boldsymbol{r}_i$, and $V_{\alpha\alpha}$ an $\alpha+\alpha$ potential. A phenomenological 3α potential $V_{\alpha\alpha\alpha}$ is in general included in this Hamiltonian [34, 20]. Although 3-body continuum calculations become feasible with microscopic cluster models [35] where the internal structure of the particles is taken into account, their application is currently limited to lighter systems such as $\alpha+n+n$. Here, we focus on non-microscopic approaches where the α internal structure is neglected. Essentially three types of $\alpha+\alpha$ potentials are available:

- *Local deep potentials*. In this variant, the potentials present additional (unphysical) bound states, which simulate the Pauli forbidden states [36]. Pauli forbidden states stem from antisymmetrization effects. They show up naturally in microscopic cluster theories where the antisymmetrization between all nucleons is exactly taken into account, and where the internal wave functions of the clusters are defined in the shell model with a common oscillator parameter b. In that case, Pauli forbidden

states are expressed as harmonic-oscillator functions. For the $\alpha + \alpha$ system, the Buck potential [24] is known to accurately reproduce the phase shifts up to 20 MeV. The use of deep potentials in two-body problems is very simple, as forbidden states are eliminated automatically. For multi-body systems, however, the situation is more complicated as these two-body forbidden states introduce spurious states. Consequently, the total wave function must be orthogonalized to the two-body forbidden states $\varphi_k(r)$. This is achieved by adding, in the Hamiltonian (1), the projector [37]

$$P = \Lambda \sum_{k=1}^{n} \mid \varphi_k(\boldsymbol{r})\rangle\langle\varphi_k(\boldsymbol{r}) \mid, \tag{2}$$

for each $\alpha + \alpha$ pair. In Eq. (2), $\boldsymbol{r}$ is the $\alpha - \alpha$ coordinate, and Λ is a constant chosen large enough (typically $\Lambda \sim 10^4 - 10^5$ MeV) to move the forbidden states in the high-energy region. This projector makes the $\alpha + \alpha$ interaction non local. The number of forbidden states n depends on the system and on the angular momentum ℓ ($2n + \ell = 8$ for $\alpha + \alpha$).

For the 3α system, the use of the pseudo-potential method provides controversial results [38, 26, 39]. As the forbidden states $\varphi_k(r)$ stem from microscopic arguments, it seems natural to take harmonic-oscillator functions with an appropriate oscillator parameter (for example, deduced from the radius of the α particle). This procedure provides an *overbinding* of the ^{12}C ground state [26, 25]. On the other hand, an alternative is to use the deep states generated by the potentials as forbidden states, which leads to an *underbinding* of the ^{12}C ground state [38, 40]. This paradox was clarified by Matsumura *et al.* [27] who showed that removing the forbidden states of the potential is inconsistent with microscopic arguments.

- *Local shallow potentials.* These potentials do not contain forbidden states. A typical example is the Ali-Bodmer potential [41], which presents a repulsive core at low angular momenta. The Ali-Bodmer potential provides a good fit of the $\alpha + \alpha$ phase shifts. In fact, it was shown that deep and shallow potentials are related to each other by a supersymmetry transform [42], and are therefore phase equivalent. In shallow potentials, microscopic effects are simulated by a repulsive core at short distances. This variant is of course easier to use for multi-α systems as spurious states do not show up and there is no need for the projector (2). It has been adopted by Alvarez-Rodriguez *et al.* [34] to investigate low-lying ^{12}C resonances. According to the work of Matsumura *et al.* [27], it is however not clear whether this potential is well adapted to multi-particle systems or not.
- *Non-local potentials.* The $\alpha + \alpha$ potentials derived from microscopic cluster models are non local [43]. Recently some progress has been made to implement non-local potentials in three-body calculations [44, 45], but they are currently limited to bound states. Their use in variational calculations is possible, but owing to the many problems encountered in the calculation of 3-body phase shifts, they are quite difficult to adapt to scattering theories.

Table 1. Theoretical properties (energy E_R, width Γ, in MeV) of 0^+ and 2^+ resonances in various models.

J^π	Ref. [46][a]	Ref. [18][b]	Ref. [20][c]	Ref. [34][d]
0^+		4.7, 1.0	1.66, 1.48	3.95, 1.0
			4.58, 1.1	
2^+	$2.6 \pm 0.3, 1.0 \pm 0.3$	2.1, 0.8	2.28, 1.1	1.38, 0.132
		4.9, 0.9	5.14, 1.9	4.48, 1.086
				6.49, 2.250

[a] Microscopic model with the ACCC method.
[b] Microscopic model with the CSM method and α+^{8}Be phase shifts.
[c] Non-microscopic model with a deep $\alpha + \alpha$ potential and a repulsive 3α force.
[d] Non-microscopic model with the Ali-Bodmer $\alpha + \alpha$ potential and an attractive 3α force.

In Table 1, we present recent theoretical results on 3α resonances. We limit the discussion to 0^+ and 2^+ states. In Ref. [34], the authors use the Ali-Bodmer potential [41] with an attractive 3α interaction to fit the experimental ground-state energy on the first 0^+ state of the model. The continuum is treated with the CSM method. Although the rotation angle is rather small, several additional resonances, not known experimentally, are found. In particular, a narrow 2^+ state is obtained at $E_{cm} = 1.38$ MeV. The use of a larger rotation angle may still provide more resonances. As shown by Matsumura *et al.* [27], the treatment of forbidden states in the 3α system is a delicate problem. The authors recommend to use deep $\alpha + \alpha$ potentials with forbidden states consistent with the underlying microscopic model. From recent works on the 3α system, the 3-body potential seems to be repulsive [20, 44], which is not consistent with the choice adopted in Ref. [34]. The repulsive nature of the 3α interaction is supported by microscopic theories where, starting from a nucleon-nucleon force fitting the $\alpha + \alpha$ phase shifts, the 3α ground state is overbound [9, 18, 25].

Kurokawa and Katō [20] use a similar 3α model complemented by the CSM method. In contrast with Ref. [34], the $\alpha+\alpha$ potential is deep [47], and a repulsive 3α interaction must be used to compensate the ground state overbinding. Concerning 0^+ resonances, Kurokawa and Katō find a state near 4 MeV, in agreement with Ref. [34]. However, an additional broad resonance is found near 1.7 MeV ($\Gamma = 1.48$ MeV). This state could not be seen in Ref. [34] owing to the small rotation angle used in the CSM. For the 2^+ resonances, the results are very different. This may be related to the different $\alpha + \alpha$ potentials used in these references.

Funaki *et al.* [46] and Arai [18] investigate the 3α continuum in a microscopic three-cluster model with different basis functions. A microscopic approach avoids the choice of an $\alpha + \alpha$ potential since the model is based on a nucleon-nucleon force. However, NN interactions fitting the $\alpha + \alpha$ phase shifts provide ^{12}C low lying states too strongly bound. The properties of the 0^+_2 Hoyle state are well reproduced, in agreement with the interpretation of this resonance as a cluster state. Funaki *et al.* [46] use the ACCC

method to derive resonance properties. This method is known to require a high accuracy of the basis [48] and becomes unstable for broad resonances. The authors only find a 2_2^+ resonance near 2.6 MeV.

Arai [18] uses the CSM and finds a broad 0^+ state near 5 MeV. The properties of this resonance agree reasonably well within the different models. The two additional 2^+ resonances nearly correspond to the semi-microscopic results of Ref. [20]. Notice that Arai treats resonant states in two ways: with the CSM and with an R-matrix calculation of the α+^{8}Be phase shifts. Although the latter do not exactly correspond to three-body phase shifts (^{8}Be is considered as a bound system), they provide a more direct insight on the continuum properties. In particular, the 2_2^+ state is shown to have an important reduced α width and, consequently, should correspond to the 2^+ member of a rotational band based on the 0_2^+ Hoyle state.

2.2. Experimental works

For a long time, only a broad 0_3^+ state near $E_{cm} \approx 3$ MeV ($\Gamma \approx 3$ MeV) was reported in data compilations [1]. The presence of broad 0^+ states above the 3α threshold was confirmed by β-decay experiments [49, 50] from ^{12}B and ^{12}N, but precise values for the energies and widths could not be derived. It was, however, suggested that broad states may overlap with each other and make the data analysis rather complicated.

More recently, some advances have been performed in the search for a 2_2^+ state. The interest for this state is twofold. According to most theoretical predictions, the Hoyle state should be considered as the bandhead of a 0^+ rotational band. Then, the existence of a 2^+ resonance would be a strong support to cluster theories. On the other hand, this resonance should affect the triple-α reaction rate at high temperatures ($T \geq 10^9 K$). A first evidence for a 2^+ broad state was reported by Itoh *et al.* [21, 51] near $E_x \approx 9-10$ MeV. More recently, Freer *et al.* [22] performed a ^{12}C(p,p') experiment to various ^{12}C states, and conclude on a possible 2^+ state at 9.6 ± 0.1 MeV, with a width of $\Gamma = 0.6 \pm 0.1$ MeV. These properties agree nicely with microscopic predictions [9, 18]. Diget *et al.* [49] populate ^{12}C continuum states by β decay of ^{12}B and ^{12}N and investigate breakup channels. They conclude on the possible existence of a 2^+ state in the range $E_x = 10.5 - 11$ MeV.

3. Outline of the theory

3.1. The hyperspherical formalism

For 3-body systems, the Schrödinger equation associated with Eq. (1) can be solved with the hyperspherical approach [30]. The hyperradius ρ and hyperangle α are deduced from the scaled Jacobi coordinates

$$\begin{aligned} \boldsymbol{x} &= \sqrt{2}(\boldsymbol{r}_1 - \boldsymbol{r}_2), \\ \boldsymbol{y} &= \sqrt{\frac{32}{12}}\Big[\boldsymbol{r}_3 - \frac{\boldsymbol{r}_1 + \boldsymbol{r}_2}{2}\Big], \end{aligned} \tag{3}$$

as

$$\rho = \sqrt{x^2 + y^2},$$
$$\alpha = \arctan(y/x). \tag{4}$$

Of course, two other choices can be made for $\boldsymbol{x}$ and $\boldsymbol{y}$, with permutations of the α particles. The basis functions associated with these different choices are related to each other by a unitary transform involving the Raynal-Revai coefficients [52].

In this coordinate system, the 3-body kinetic energy involves the operator $\boldsymbol{K}^2$ which generalizes the concept of angular momentum in 2-body systems. It commutes with $\boldsymbol{\ell}_x^2$ and $\boldsymbol{\ell}_y^2$ and their common eigenfunctions $\mathcal{Y}_{\gamma K}^{JM}(\Omega_5)$ are known analytically (see Ref. [53] for details). The eigenvalue of $\boldsymbol{K}^2$ is $K(K+4)$ where the integer K is the hypermomentum quantum number. In these definitions, $\Omega_5 = (\Omega_x, \Omega_y, \alpha)$ and γ stands for $\gamma = (\ell_x, \ell_y)$ where (ℓ_x, ℓ_y) are the angular momenta associated with $(\boldsymbol{x}, \boldsymbol{y})$. The total angular momentum J results from the coupling of ℓ_x and ℓ_y.

The wave function in partial wave $J\pi$ is then expanded over hyperspherical harmonics as

$$\Psi^{JM\pi}(\rho, \Omega_5) = \rho^{-5/2} \sum_{\gamma K} \chi_{\gamma K}^{J\pi}(\rho)\ \mathcal{Y}_{\gamma K}^{JM}(\Omega_5), \tag{5}$$

where the hyperradial functions $\chi_{\gamma K}^{J\pi}(\rho)$ have to be determined. The Schrödinger equation is replaced by a system of coupled differential equations

$$\left[-\frac{\hbar^2}{2m_N}\left(\frac{d^2}{d\rho^2} - \frac{(K+3/2)(K+5/2)}{\rho^2}\right) - E\right] \chi_{\gamma K}^{J\pi}(\rho) + \sum_{K'\gamma'} V_{K\gamma,K'\gamma'}^{J\pi}(\rho)\, \chi_{\gamma' K'}^{J\pi}(\rho) = 0, \tag{6}$$

where the matrix elements of the 2-body potentials are defined as

$$V_{K\gamma,K'\gamma'}^{J\pi}(\rho) = \langle \mathcal{Y}_{\gamma K}^{JM}(\Omega_5) | \sum_{i>j=1}^{3} V_{\alpha\alpha}(\boldsymbol{r}_j - \boldsymbol{r}_i) | \mathcal{Y}_{\gamma' K'}^{JM}(\Omega_5) \rangle. \tag{7}$$

In Eq. (7), the integrals over Ω_x and Ω_y are performed analytically, whereas a numerical quadrature is used for the integral over the hyperangle α. With the Raynal-Revai coefficients [52] the evaluation of the potential matrix elements (7) is rather easy. In Eq. (5), a truncation must be done in the summation over K; the maximum K value is denoted as $K_{\max}$. The number of γK components increases rapidly when $K_{\max}$ increases.

In Ref. [54], we have solved the system (6) with the Lagrange-mesh method [55]. Each hyperradial wave function is expanded as

$$\chi_{\gamma K}^{J\pi}(\rho) = \sum_{i=1}^{N} c_{\gamma K i}^{J\pi}\, \varphi_i(\rho), \tag{8}$$

where $\varphi_i(\rho)$ are N Lagrange functions and $c_{\gamma K i}^{J\pi}$ variational coefficients. The use of these basis functions greatly simplifies the calculations, since matrix elements computed at the Gauss approximation do not need any numerical integral. In spite of its simplicity the method is very accurate (see Ref. [55] for futher detail).

The 3α wave function must be symmetrized under α exchanges. In other words, the wave function (5) must satisfy

$$\mathcal{S}\Psi^{JM\pi} = \frac{1}{3}(1 + S_{13} + S_{23})\Psi^{JM\pi} = \Psi^{JM\pi}, \tag{9}$$

where S_{ij} is the exchange operator between particles i and j. Symmetry between particles 1 and 2 is automatic, since only even partial waves ℓ_x are included in expansion (5). Eq. (9) can be easily solved with the help of the Raynal-Revai coefficients. For a given K value, operator $\mathcal{S}$ is diagonalized, which provides eigenvalues 1 and 0. Only the former eigenstates are kept in the basis.

3.2. The R-matrix theory for 3-body continuum states

The treatment of three-body continuum states ($E > 0$), with exact three-body asymptotic conditions, is recent [56, 31]. In the R-matrix method [57, 58], the configuration space is divided into two regions: the internal region (with radius a) where the nuclear force must be taken into account, and the external region where the potentials have reached their asymptotic (Coulomb) behaviour. Consequently the solutions of the system (6) are written as,

$$\chi^{J\pi}_{\gamma K,\mathrm{int}}(\rho) = \sum_{i=1}^{N} c^{J\pi}_{\gamma K i}\,\varphi_i(\rho), \text{ for } \rho < a. \tag{10}$$

In the external region, potentials (7) are assumed to be given by their asymptotic form. As discussed in Refs. [59, 31], the Coulomb part of potential (7) tends to

$$V^{J\pi,\mathrm{Coul}}_{K\gamma,K'\gamma'}(\rho) \to z^{J\pi}_{K\gamma,K'\gamma'}\frac{e^2}{\rho}, \tag{11}$$

where matrix $\boldsymbol{z}^{J\pi}$ represents 3-body effective charges. They are computed from the 2-body Coulomb potentials. An example is given in Table 2 for $J = 0^+$, and for $K \leq 8$. In most cases the non-diagonal elements are small compared to the diagonal terms. Neglecting non-diagonal terms provides uncoupled solutions of Eq. (6). Accordingly, the external solution reads, for an entrance channel γ',

$$\chi^{J\pi}_{\gamma K,\mathrm{ext}}(\rho) = C^{J\pi}_{\gamma K}\left[H^{-}_{\gamma K}(k\rho)\delta_{\gamma\gamma'}\delta_{KK'} - U^{J\pi}_{\gamma K,\gamma' K'}H^{+}_{\gamma K}(k\rho)\right], \tag{12}$$

where $k = \sqrt{2m_N E/\hbar^2}$ is the three-body wave number (m_N is the nucleon mass). In Eq. (12), $C^{J\pi}_{\gamma K}$ is a normalization coefficient, $\boldsymbol{U}^{J\pi}$ is the three-body collision matrix and the incoming and outgoing functions $H^{\pm}_{\gamma K}(x)$ are defined as

$$H^{\pm}_{\gamma K}(x) = G_{K+\frac{3}{2}}(\eta_{\gamma K}, x) \pm iF_{K+\frac{3}{2}}(\eta_{\gamma K}, x), \tag{13}$$

where the Sommerfeld parameters $\eta_{\gamma K}$ are given by

$$\eta_{\gamma K} = z^{J\pi}_{\gamma K,\gamma K}\frac{m_N e^2}{\hbar^2 k}, \tag{14}$$

and therefore depend on the channel.

According to the R-matrix formalism, matrix elements between basis functions $\varphi_i(\rho)$ must be computed over the internal region. Then the use of the Bloch operator

Table 2. Effective charges $z^{J\pi}_{K\gamma,K'\gamma'}$ [see Eq. (11)] for $J=0^+$ ($\ell_x=\ell_y, \ell'_x=\ell'_y$).

	K,ℓ_x							
K',ℓ'_x	0,0	4,0	6,0	8,0	4,2	6,2	8,2	8,4
0,0	28.81	2.47	−2.75	0.88	3.50	2.75	1.05	1.40
4,0	2.47	22.05	−4.92	5.36	6.02	−0.65	−0.08	0.63
6,0	−2.75	−4.92	27.01	−5.56	−1.05	−9.00	−1.69	0.46
8,2	0.88	5.36	−5.56	23.07	−1.13	−2.82	1.87	3.40
4,2	3.50	6.02	−1.05	−1.13	26.31	4.99	3.24	3.83
6.2	2.75	−0.65	−9.00	−2.82	4.99	27.01	1.58	4.85
8,2	1.05	−0.08	−1.69	1.87	3.24	1.58	19.72	7.06
8,4	1.40	0.63	0.46	3.40	3.83	4.85	7.06	23.37

[58] makes the kinetic energy Hermitian, and ensures the continuity of the derivative of the wave function at $\rho=a$. The matching between the internal and external solutions provides the collision matrix $\boldsymbol{U}^{J\pi}$. A strong test of the calculation is that the collision matrix should not depend on the channel radius a and on the number N of basis functions, provided that they are large enough to meet the R-matrix requirements.

As shown in Ref. [31], an important issue in 3-body scattering states is the long range of the three-body potential (7). At large distances, the nuclear part of this potential behaves as

$$V^{J\pi,\mathrm{Nuc}}_{K\gamma,K'\gamma'}(\rho) \underset{\rho\to\infty}{\longrightarrow} \frac{v^{J\pi}_{0,K\gamma,K'\gamma'}}{\rho^3}, \tag{15}$$

even with short-range two-body interactions. This property arises from the definition of the hyperspherical coordinates. Even for large ρ values, two particles can still be close to each other and strongly interact. Constants $v^{J\pi}_{0,K\gamma,K'\gamma'}$ can be quite large (examples are given in Ref. [31]). For this reason, the R-matrix radius takes unusually large values (typically $a\sim 800-1000$ fm for the 3α system) to ensure that potential (15) is negligible compared with the centrifugal and Coulomb terms (for comparison, typical values in two-body scattering is $a\approx 10$ fm [58]).

To avoid huge basis sizes, propagation techniques are necessary. We follow the method of Ref. [31], where the R-matrix is computed at some channel radius a_0 with the basis (10). Typical values of a_0 are $a_0\approx 30-40$ fm with $N\approx 40-50$ basis functions. At this radius the nuclear interaction is far from being negligible, and the asymptotic form (12) is not valid. Consequently the R-matrix determined at a_0 is propagated up to $\rho=a$ with the Numerov algorithm. This technique is based on an analytical approximation of the nuclear potential in the region $a_0\le\rho\le a$

$$V^{J\pi,\mathrm{Nuc}}_{\gamma K,\gamma' K'}(\rho) \approx \sum_{k=0}^{\infty} \frac{v_k}{\rho^{2k+3}}, \tag{16}$$

where coefficients v_k are computed from integrals of the two-body potentials. They depend on the different quantum numbers. Expansion (16) is a generalization of the asymptotic behaviour (15). In practice the summation over index k is truncated at

some $k_{\max}$ value, which can be quite large in the 3α system to achieve a good accuracry ($k_{\max} \approx 30 - 40$).

This formalism is limited to local potentials, and is not valid for non-local interactions, where expansion (16) must be adapted. Consequently current calculations are restricted to local $\alpha + \alpha$ interactions. This means that deep potentials cannot be used since the associated projector (2) is non-local. Only shallow potentials, such as the Ali-Bodmer potential, can be currently considered to derive three-body phase shifts. Further developments are still necessary to deal with non-local interactions in the R-matrix formalism.

The collision matrix may involve many channels, in particular for large $K_{\max}$ values, and is in general analyzed through its eigenvalues. In addition, the Coulomb contribution should be removed from the eigenphases. As explained in Ref. [31] this is achieved by evaluating the pure Coulomb collision matrix $\boldsymbol{U}_C^{J\pi}$ (the nuclear potential is set to zero). Then the nuclear collision matrix $\boldsymbol{U}_N^{J\pi}$ is defined as

$$\boldsymbol{U}^{J\pi} = \left(\boldsymbol{U}_C^{J\pi}\right)^{1/2} \boldsymbol{U}_N^{J\pi} \left(\boldsymbol{U}_C^{J\pi}\right)^{1/2}. \tag{17}$$

Matrix $\boldsymbol{U}_N^{J\pi}$ is easily shown to be symmetric and unitary. Its eigenvalues can therefore be written as

$$u_{N,i}^{J\pi} = \exp(2i\delta_i^{J\pi}), \tag{18}$$

where the eigenphases $\delta_i^{J\pi}$ are real. The number of eigenphases is of course equal to the number of channels γK.

3.3. The Complex Scaling method

The R-matrix theory provides 3-body wave functions at any scattering energy. The calculation of the phase shifts is obviously the optimal way to investigate the continuum, and in particular broad resonances. In practice, however, dealing with the continuum is an heavy task, especially for three-body systems. As mentioned before, only shallow local potentials can be currently employed. For these reasons a number of approximate methods have been developed. The common idea is to derive resonance properties (energy and width) from bound-state calculations, which only requires slight modifications of well mastered techniques. In the CSM [60, 61, 28, 62], the space radial coordinate r and the momentum p are transformed as

$$\begin{aligned} U(\theta)r &= r\exp(i\theta), \\ U(\theta)p &= p\exp(-i\theta), \end{aligned} \tag{19}$$

where θ is the scaling angle. Under this transformation the Schrödinger equation reads

$$H(\theta)\Psi(\theta) = E(\theta)\Psi(\theta), \tag{20}$$

with

$$H(\theta) = U(\theta)HU(\theta)^{-1}. \tag{21}$$

The diagonalization of $H(\theta)$ with square-integrable functions can be done in various bases, such as Gaussian [38] or Lagrange basis [54]. The ABC theorem [60, 61] demonstrates that this diagonalization provides continuum states along straight lines in the complex plane, rotated by an angle 2θ from the positive real axis. On the contrary, resonant states are not modified under variations of θ. The resonance energy E_R and width Γ are determined from

$$E(\theta) = E_R - i\Gamma/2, \tag{22}$$

and are independent (at the numerical accuracy of the calculation) of θ. The main interest for the CSM is its simplicity. Standard three-body codes can be easily adapted by introducing transformation (17), and by diagonalizing a complex matrix. Of course broad resonances require large rotation angles ($\tan 2\theta \geq \Gamma/2E_R$). A limitation of the CSM is that the potential must be analytic. In addition, only the total width of a resonance can be determined. In coupled-channel calculations the partial widths in the different channels cannot be computed individually. Further detail, and in particular applications to three-body systems in nuclear physics, can be found in Ref. [62].

4. Results

4.1. Conditions of the calculations

The calculations are performed with two $\alpha + \alpha$ potentials widely used in the literature: the shallow Ali-Bodmer (AB) potential [41] (ℓ-dependent potential d), and the deep potential of Buck *et al.* (BFW) [24]. Both interactions reproduce fairly well the $\alpha + \alpha$ phase shifts up to $E \approx 20$ MeV, i.e. below the proton threshold in ^{8}Be. As the BFW potential introduces spurious 3α states in the ^{12}C spectrum, the projector (2) is used to remove $\alpha + \alpha$ Pauli forbidden states. According to Ref. [27], the two-body forbidden states are defined as harmonic-oscillator orbitals. The oscillator parameter b is chosen as in Ref. [44], i.e. $b = 1.395$ fm. The constant Λ is taken as 10^4 MeV, but all results are insensitive to that choice provided it is large enough ($\Lambda \gtrsim 10^3$ MeV).

As discussed in Section 2, both potentials have been used by several authors to investigate ^{12}C bound states. It is well known that a 3α potential must be introduced to reproduce the ground-state energy. According to Ref. [34], we choose the three-body interaction as

$$V_{\alpha\alpha\alpha}(\rho) = v_3 \exp(-(\rho/\rho_3)^2), \tag{23}$$

with the range $\rho_3 = 6$ fm. This phenomenological potential only depends on the hyperradius, and can be easily introduced in the hyperspherical equations (6). The amplitude v_3 is adjusted, for each potential and angular momentum, on the experimental energies. The values are given in Table 3, which confirms that the 3α potential must be attractive for the AB potential, and repulsive for the BFW potential. For the AB potential, v_3 strongly depends on angular momentum, whereas this dependence is weak for the BFW potential.

Table 3. Amplitude v_3 (in MeV) of the 3α potential (23) for the AB and BFW $\alpha+\alpha$ interactions.

J^π	AB	BFW
0^+	-22.0	23.3
2^+	-11.9	25.2

Calculations with the CSM method are performed with Lagrange-Laguerre basis functions [54] (typically $N = 50$), and a scaling parameter $h = 0.3$ fm. The R-matrix calculations (see Ref. [31] for detail) are performed with 50 Lagrange-Legendre functions with a channel radius $a_0 = 40$ fm. The R-matrix is then propagated up to $a = 1000$ fm, where the wave functions have reached their asymptotic behaviour (12). The sensitivity with respect to these parameters is quite low (less than 1° in the phase shifts). As continuum states are known to converge slowly in the hyperspherical formalism [32, 56, 31], large $K_{\max}$ values must be used in the expansion (5). However, our aim is not to derive fully converged values, but to investigate qualitatively the ^{12}C spectrum above the 3α threshold. For $J = 0^+$, we use $K_{\max} = 44$, which represents 144 values of quantum numbers γK. For $J = 2^+$, the number of channels is of course larger, and the $K_{\max}$ value has to be reduced. We use $K_{\max} = 24$, which represents 120 channels.

4.2. Continuum states with the AB potential

We start the analysis without three-body potential ($v_3 = 0$). In Fig. 1, we show the 0^+ eigenphases (18) and the corresponding complex energies (22). Here and in the following, bound states ($\mathrm{Re}(E) < 0$) are not shown in the figures, but are given in Table 4. We analyze the convergence with respect to $K_{\max}$ ($K_{\max} = 36, 40$ and 44 are presented). The first three eigenphases ($i = 1, 2, 3$ in Eq. (18)) present a narrow resonance between 1 and 2 MeV. These resonances are less and less narrow when energy increases. Their energy and width deduced from the phase shifts are very close to those obtained with the CSM calculations, but the phase shifts also provide information off resonances. The bound-state and resonance energies for $K_{\max} = 44$ are displayed in Table 4 which shows that the lowest 0^+ state is found at -1.60 MeV. The underbinding of ^{12}C with the AB potential is well known [5, 40], and can be solved by using an attractive three-body interaction.

The $J = 0^+$ eigenphases and complex energies with the 3α potentials of Table 3 are displayed in Fig. 2, for $K_{\max} = 44$. To check the stability of physical resonances with respect to the scaling angle, we use two values: $\theta = 0.25$ and $\theta = 0.30$. Several states are stable and can also be observed in the eigenphases. The second 0^+ state is located at -0.12 MeV (see Table 4) but, as for $v_3 = 0$, several additional resonances between 0.5 and 2 MeV are observed in the eigenphases, and confirmed by the CSM method. A further narrow state near 3 MeV ($\Gamma \approx 0.4$ MeV) is obtained.

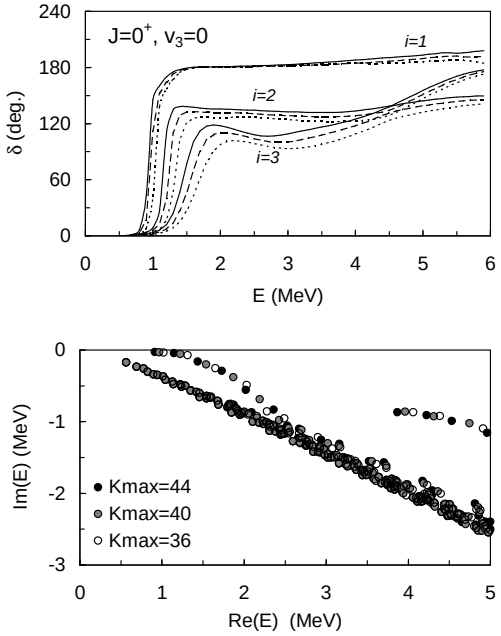

Figure 1. Three-α phase shifts (upper panel) and complex energies (lower panel, $\theta = 0.25$) for the Ali-Bodmer potential ($J = 0^+$) without 3-body potential ($v_3 = 0$). In the phase shifts, dotted, dashed and solid lines correspond to $K_{\max} = 36, 40$ and 44, respectively.

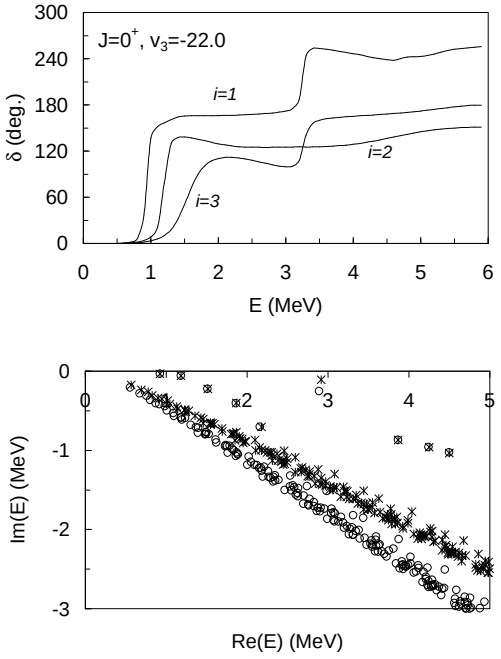

Figure 2. Three-α phase shifts (upper panel) and complex energies (lower panel) for the Ali-Bodmer potential ($J = 0^+$), with a 3-body potential $v_3 = -22.0$ MeV. Complex energies are displayed for two angles: $\theta = 0.25$ (crosses), and $\theta = 0.30$ (circles).

Table 4. Energies E_R and widths Γ (in MeV) with the AB potential.

$J = 0^+$		$J = 2^+$	
$v_3 = 0$	$v_3 = -22.0$ MeV	$v_3 = 0$	$v_3 = -11.9$ MeV
-1.60	-7.16	$0.46, 0.003$	-3.00
$0.92, 0.06$	-0.12	$1.6, 0.2$	$1.6, 0.2$
$1.15, 0.09$	$0.93, 0.07$	$2.3, 0.6$	$1.8, 0.2$
$1.4, 0.3$	$1.2, 0.1$		$2.4, 1.2$
$1.7, 0.6$	$1.5, 0.5$		$3.9, 0.03$
	$1.9, 0.8$		
	$3.1, 0.4$		

The results for $J = 2^+$ are presented in Fig. 3. Without the 3α potential the lowest 2^+ state is unbound (see Table 4), and would show up as a sharp resonance in the phase shifts. The CSM analysis shows that several resonances are insensitive to the θ value, and can be observed in the phase shifts. With $v_3 = -11.9$ MeV, a narrow state is found near 4 MeV.

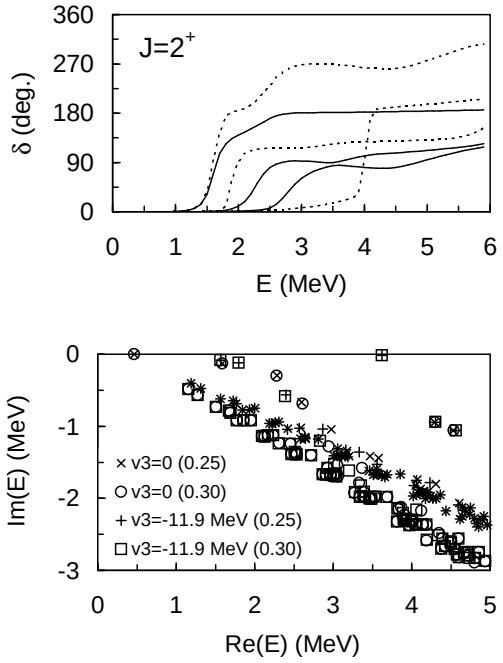

Figure 3. Continuum states for $J = 2^+$ with the Ali-Bodmer potential. Upper panel: three-α phase shifts (solid lines: $v_3 = 0$, dotted lines: $v_3 = -11.9$ MeV). Lower panel: complex energies for $v_3 = 0$ and $v_3 = -11.9$ MeV with two scaling angles ($\theta = 0.25$ and 0.30).

The present analysis may help in understanding the recent results of Ogata *et al.* on the 3α process within the CDCC framework [15]. Although the models are different, both provide three-body wave functions which should tend to the exact solution of the Schrödinger equation. Ogata *et al.* find a triple-α reaction rate about 10^{20} times larger

than previously accepted at a temperature $T = 10^7$ K. This huge factor, inconsistent with stellar models [63], might be explained by additional 0^+ resonances. The $\alpha + \alpha$ potential used by Ogata *et al.* is very similar to the Ali-Bodmer potential, and is also expected to give rise to additional resonances in the CDCC approach. This would explain the unexpectedly large factor obtained in the CDCC 3α reaction rate.

4.3. Continuum states with the BFW potential

As explained in Section 3.2, the analysis of continuum states with a deep potential is limited to the CSM. The reason is that the projector over forbidden states (2) introduces non-locality in the three-body equations, even at large ρ values.

The complex energies for $J = 0^+$ and 2^+ are presented in Fig. 4 for two scaling angles (see also Table 5). Without a three-body force, the low-lying states are overbound. This result is well known [5, 26]. In these conditions, narrow resonances show up near $E = 1.45$ MeV ($J = 0^+$) and $E = 1.84$ MeV ($J = 2^+$). Introducing a 3α potential moves the 0_2^+ Hoyle state slightly above the experimental energy ($E = 0.38$ MeV) and gives rise to 0^+ broad resonances near 2.3 and 4.8 MeV. These states are quite stable when changing the scaling angle (see Fig. 4). A similar behaviour is obtained for $J = 2^+$. With $v_3 = 25.1$ MeV, we obtain a broad resonance ($\Gamma = 0.8$ MeV) at $E_R = 3.6$ MeV.

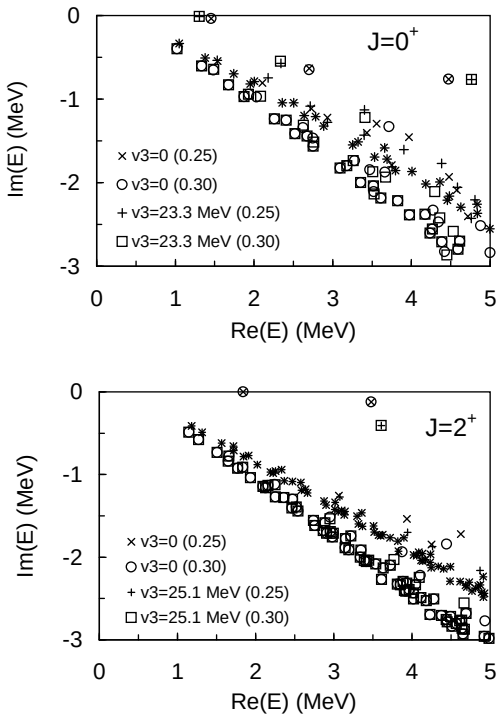

Figure 4. Complex energies with the BFW potential for $J = 2^+$ with and without a 3α potential.

Our results with the BFW potential are qualitatively in agreement with those of Kurokawa and Katō [20] (see Table 1), who use a deep potential derived from a folding

model. Our 0_3^+ and 2_2^+ broad resonances are at slightly higher energies. The present calculations suggest that the description of the 3α continuum is very sensitive to the type of potential. The deep BFW potential provides results consistent with experiment, in contrast with shallow potentials, such as the AB interaction, which predict several narrow states, not supported by experiment.

Table 5. Energies E_R and widths Γ (in MeV) with the BFW potential.

$J = 0^+$		$J = 2^+$	
$v_3 = 0$	$v_3 = 23.3$ MeV	$v_3 = 0$	$v_3 = 25.1$ MeV
-20.62	-7.18	-17.17	-3.01
-1.26	$1.31, 0.02$	$1.84, 0.0017$	$3.6, 0.8$
$1.45, 0.07$	$2.3, 1.1$	$3.5, 0.2$	
$2.7, 1.3$	$4.8, 1.5$		
$4.5, 1.5$			

5. Conclusion

The theoretical study of the 3α continuum represents a typical example of open problem. Our goal is of course not to provide a definite solution to the 3α problem, but to draw attention on the strong sensitivity of continuum states on the $\alpha + \alpha$ potential. Although the physics of ^{12}C above the α threshold is an important issue in nuclear physics and in nuclear astrophysics, it remains unclear. A rigorous treatment of the continuum requires the calculation of the phase shifts which provides, not only resonance properties, but also information on the 3α process off resonances. Until now, three-body continuum calculations were essentially limited to the $\alpha + n + n$ system, where the phase shifts suggest broad resonances at low energies. In the 3α system, the phase shifts computed with the AB potential present several narrow resonances, which do not have experimental counterparts. The existence of such narrow states could be an explanation for the huge triple α reaction rate of Ogata *et al.* [15], who use an $\alpha + \alpha$ potential very similar to the AB potential.

Of course R-matrix calculations can only be performed by neglecting non-diagonal terms of the Coulomb interaction at large distances (see the discussion in Section 3.2). However, the consistency between the phase shift analysis and the CSM results, as well as the stability of the phase shifts against variations of different parameters (R-matrix radii a_0 and a, number of basis functions) indicate that this approximation should not affect the conclusions.

An important output of our work is the sensitivity of the 3α continuum properties with respect to the choice of the $\alpha + \alpha$ potential. This result is not surprising as the bound-state spectrum is also dependent on the potential (see for example Ref. [5]). Calculations with the deep BFW potential are currently limited to the CSM method, but provide resonance energies which significantly differ from the AB interaction. In

addition to the $0_1^+, 0_2^+$ and 2_1^+ states, only broad resonances beyond 3 MeV are found. The 2_2^+ resonance might correspond to the new state observed in recent experiments [22, 49].

Improvements of the present study could be done by using non-local potentials. Recent works propose non-local $\alpha+\alpha$ interactions derived either from the RGM kernels [44] or from a phenomenological approach [45]. In particular the potential of Ref. [45] reproduces simultaneously the experimental energies of the 0_1^+ and 0_2^+ states in a 3α description of ^{12}C. However performing continuum calculations with non-local potentials strongly increases the complexity of the model, in particular for the R-matrix theory. An alternative approach is to use microscopic cluster models, which do not rely on $\alpha+\alpha$ potentials, but on a nucleon-nucleon interaction. Calculations of the $\alpha+^8$Be have been performed [9, 18], but the determination of the 3α phase shifts in this framework is still a challenge for the future.

Acknowledgments

This text presents research results of the IAP programme P6/23 initiated by the Belgian-state Federal Services for Scientific, Technical and Cultural Affairs.

References

[1] Ajzenberg-Selove F 1990 *Nucl. Phys. A* **506** 1
[2] Karataglidis S, Dortmans P J, Amos K and de Swiniarski R 1995 *Phys. Rev. C* **52** 861
[3] Navrátil P and Ormand W E 2003 *Phys. Rev. C* **68** 034305
[4] Navrátil P, Vary J P and Barrett B R 2000 *Phys. Rev. Lett.* **84** 5728
[5] Horiuchi H 1975 *Prog. Theor. Phys.* **53** 447
[6] Uegaki E, Okabe S, Abe Y and Tanaka H 1977 *Prog. Theor. Phys.* **57** 1262
[7] Fujiwara Y, Horiuchi H, Ikeda K, Kamimura M, Katō K, Suzuki Y and Uegaki E 1980 *Prog. Theor. Phys. Suppl.* **68** 29
[8] Kamimura M 1981 *Nucl. Phys. A* **351** 456
[9] Descouvemont P and Baye D 1987 *Nucl. Phys. A* **463** 629
[10] Chernykh M, Feldmeier H, Neff T, von Neumann-Cosel P and Richter A 2007 *Phys. Rev. Lett.* **98** 032501
[11] Hoyle F 1954 *Astrophys. J. Suppl.* **1** 121
[12] Dunbar D N F, Pixley R E, Wenzel W A and Whaling W 1953 *Phys. Rev.* **92** 649
[13] Cook C W, Fowler W A, Lauritsen C C and Lauritsen T 1957 *Phys. Rev.* **107** 508
[14] Nomoto K, Thielemann F K and Miyaji S 1985 *Astron. Astrophys.* **149** 239
[15] Ogata K, Kan M and Kamimura M 2009 *Prog. Theor. Phys.* **122** 1055
[16] Tohsaki A, Horiuchi H, Schuck P and Röpke G 2001 *Phys. Rev. Lett.* **87** 192501
[17] Funaki Y, Tohsaki A, Horiuchi H, Schuck P and Röpke G 2006 *Eur. J. Phys. A* **28** 259
[18] Arai K 2006 *Phys. Rev. C* **74** 064311
[19] Ikeda K, Takigawa N and Horiuchi H 1968 *Prog. Theo. Phys. Suppl., Extra Number* 464
[20] Kurokawa C and Katō K 2007 *Nucl. Phys. A* **792** 87
[21] Itoh M *et al.* 2004 *Nucl. Phys. A* **738** 268
[22] Freer M *et al.* 2009 *Phys. Rev. C* **80** 041303
[23] Wildermuth K and Tang Y C 1977 *A Unified Theory of the Nucleus* (Vieweg, Braunschweig)
[24] Buck B, Friedrich H and Wheatley C 1977 *Nucl. Phys. A* **275** 246

[25] Theeten M, Matsumura H, Orabi M, Baye D, Descouvemont P, Fujiwara Y and Suzuki Y 2007 *Phys. Rev. C* **76** 054003
[26] Fujiwara Y, Kohno M and Suzuki Y 2004 *Few-Body Syst.* **34** 237
[27] Matsumura H, Orabi M, Suzuki Y and Fujiwara Y 2006 *Nucl. Phys. A* **776** 1
[28] Ho Y K 1983 *Phys. Rep.* **99** 1
[29] Kukulin V I, Krasnopolsky V M and Horăćek J 1989 *Theory of Resonances, Principles and Applications* (Kluwer Academic)
[30] Lin C D 1995 *Phys. Rep.* **257** 1
[31] Descouvemont P, Tursunov E M and Baye D 2006 *Nucl. Phys. A* **765** 370
[32] Fedorov D V and Jensen A S 1996 *Phys. Lett. B* **389** 63
[33] Danilin B V, Thompson I J, Vaagen J S and Zhukov M V 1998 *Nucl. Phys. A* **632** 383
[34] Alvarez-Rodriguez R, Garrido E, Jensen A S, Fedorov D V and Fynbo H O U 2007 *Eur. J. Phys. A* **31** 303
[35] Damman A and Descouvemont P 2009 *Phys. Rev. C* **80** 044310
[36] Saito S 1969 *Prog. Theor. Phys.* **41** 705
[37] Kukulin V I and Pomerantsev V N 1978 *Ann. Phys.* **111** 330
[38] Tursunov E M 2001 *J. Phys. G* **27** 1381
[39] Fujiwara Y, Suzuki Y and Kohno M 2004 *Phys. Rev. C* **69** 037002
[40] Tursunov E M, Baye D and Descouvemont P 2003 *Nucl. Phys. A* **723** 365
[41] Ali S and Bodmer A R 1966 *Nucl. Phys.* **80** 99
[42] Baye D 1987 *Phys. Rev. Lett.* **58** 2738
[43] Horiuchi H 1977 *Prog. Theor. Phys. Suppl.* **62** 90
[44] Suzuki Y, Matsumura H, Orabi M, Fujiwara Y, Descouvemont P, Theeten M and Baye D 2008 *Phys. Lett. B* **659** 160
[45] Papp Z and Moszkowski S 2008 *Mod. Phys. Lett. B* **22** 2201
[46] Funaki Y, Tohsaki A, Horiuchi H, Schuck P and Röpke G 2005 *Eur. J. Phys. A* **24** 321
[47] Schmid E W and Wildermuth K 1961 *Nucl. Phys.* **26** 463
[48] Tanaka N, Suzuki Y, Varga K and Lovas R G 1999 *Phys. Rev. C* **59** 1391
[49] Diget C A *et al.* 2009 *Phys. Rev. C* **80** 034316
[50] Fynbo H O U *et al.* 2005 *Nature* **433** 136
[51] Tamii A *et al.* 2006 *Mod. Phys. Lett. A* **21** 2367
[52] Raynal J and Revai J 1970 *Nuovo Cim. A* **39** 612
[53] Zhukov M V, Danilin B V, Fedorov D V, Bang J M, Thompson I J and Vaagen J S 1993 *Phys. Rep.* **231** 151
[54] Descouvemont P, Daniel C and Baye D 2003 *Phys. Rev. C* **67** 044309
[55] Baye D 2006 *Phys. Stat. Sol. (b)* **243** 1095
[56] Thompson I J, Danilin B V, Efros V D, Vaagen J S, Bang J M and Zhukov M V 2000 *Phys. Rev. C* **61** 024318
[57] Lane A M and Thomas R G 1958 *Rev. Mod. Phys.* **30** 257
[58] Descouvemont P and Baye D *Rep. Prog. Phys., in press*
[59] Vasilevsky V, Nesterov A V, Arickx F and Broeckhove J 2001 *Phys. Rev. C* **63** 034607
[60] Aguilar J and Combes J M 1971 *Commun. Math. Phys.* **22** 269
[61] Balslev E and Combes J M 1971 *Commun. Math. Phys.* **22** 280
[62] Aoyama S, Myo T, Katō K and Ikeda K 2006 *Prog. Theor. Phys.* **116** 1
[63] Dotter A and Paxton B 2009 *Preprint astro-ph/0905.2397*